Magnetic moments of small bimetallic clusters: Co_nMn_m

Mark B. Knickelbein
Chemistry Division, Argonne National Laboratory, Argonne, Illinois 60439, USA
(Received 11 September 2006; published 2 January 2007)

The magnetic properties of cobalt-manganese binary clusters Co_nMn_m $(n+m=11-29)$ were investigated using a Stern-Gerlach molecular beam deflection technique. One-sided beam deflections, signifying superparamagnetic behavior, were observed at temperatures of 90 K and higher. In most cases, the magnetic moments of Co_nMn_m clusters were similar to those of Co_n clusters containing the same total number of atoms. The magnitude of the magnetic moments measured are significantly larger than would be expected based on the susceptibilities of the corresponding bulk $Co_{1-x}Mn_x$ alloys.

DOI: 10.1103/PhysRevB.75.014401 PACS number(s): 82.80.Rt, 36.40.Cg, 39.10.+j

I. INTRODUCTION

Transition metal clusters containing up to $\sim 10^3$ atoms have been shown to exhibit novel magnetic behavior including nonbulklike magnetic ordering and unusually large magnetic moments.[1–8] Stern-Gerlach molecular beam deflection experiments[4,5,9–18] have proven to be useful for uncovering such behavior, as this approach allows chemically pure metal clusters to be prepared and studied with unit size resolution in isolated (i.e., matrix- and substrate-free) form. In addition to their value as tractable models for probing the size evolution of magnetic properties in reduced dimensions, small magnetic clusters are promising building blocks for magnetic nanomatericals, offering both size and composition tunability.[19]

The majority of cluster magnetism studies performed to date have involved clusters composed of a single metal. The rich and varied magnetic behavior displayed by bulk binary alloys[20] suggests that bimetallic clusters may display interesting and potentially useful magnetic properties as well. Thus far, there have been few investigations of the magnetic properties of binary clusters systems. Hihara *et al.* performed magnetic deflection studies of Co_nBi_m clusters and obtained results consistent with segregated structures consisting of ferromagnetic Co_n "cores" with a perturbing surroundings (or interface) of Bi atoms.[17] In another molecular beam deflection study, Pokrant and Becker found that Dy_nBi and Dy_nBi_2 clusters possessed higher moments than the corresponding pure Dy_n clusters, and attributed this observation to the electron withdrawing effects of the electronegative Bi heteroatoms.[16] Recently, Yin *et al.* investigated the properties of Bi_nMn_m clusters and found either ferromagnetic or ferrimagnetic coupling behavior among the manganese atoms, depending on size and composition.[21]

In this paper, we report a molecular beam deflection investigation of the magnetic properties of a binary cluster system composed of two transition metals: Co_nMn_m $(n+m=11-29)$. It is found that small Co_nMn_m clusters are superparamagnets at temperatures substantially above the ordering temperatures of the corresponding $Co_{1-x}Mn_x$ alloys, and that they possess mean per-atom moments that are substantially larger.

II. EXPERIMENTAL METHODS

The experimental methods have been provided in detail previously.[5,18] The experiment was performed using a four-stage, differentially pumped molecular beam apparatus. Clusters were produced via pulsed laser vaporization from cylindrical cobalt-manganese alloy target rods ($Co_{0.85}Mn_{0.15}$ or $Co_{0.5}Mn_{0.5}$, 99.9%, THM Inc.) housed in an aluminum source block through which helium flowed continuously at a pressure of about 10 mbar.[22] The laser vaporization source was coupled to a high aspect ratio flow tube (9 cm length $\times$0.3 cm dia.), the temperature of which can be controlled between 50 and 300 K. The residence time of the clusters within the flow tube ($\sim$4 ms) was sufficient to ensure that they were equilibrated to the flow tube temperature prior to expansion into vacuum.[23] The clusters expanded into vacuum though a 1.2 mm dia. orifice at the end of the flow tube. Under these mild expansion conditions, little supersonic cooling of the clusters' vibronic degrees of freedom is expected,[24] so that the post-expansion cluster temperature is estimated to be close (within $\sim$5 K) to that of the flow tube. The expanding jet was skimmed into a molecular beam, which passed through a gradient dipole magnet[25] capable of producing B fields of up to $\sim$1.2 T and gradients $(\partial B/\partial z)$ up to $\sim$210 T m^{-1} in the center of the gap. The clusters were then ionized with a spatially expanded ArF excimer laser ($\lambda=193$ nm), with the resulting singly ionized clusters detected mass-specifically via time-of-flight mass spectrometry. The fluence of the ionization laser was sufficiently low that neither fragmentation nor heating of the clusters occurred.[23,26,27] The mass spectrometer was operated either in space-focusing (Wiley-McLaren) mode or in position-sensitive mode[18,28,29] 0.9 m downbeam of the magnet exit slit. The position-sensitive time-of-flight (PSTOF) technique allows the spatial distributions of clusters in a molecular beam to be mapped onto the time-domain and thus recorded using a digital oscilloscope. The spatial deflections of the clusters in the beam were independently measured by quantitatively comparing the field on vs field off PSTOF peak profiles as described below.

For *differential deflection* experiments, a movable slit/beamstop assembly was positioned in the molecular beam path just prior to the TOF ionization region; in this configuration, the mass spectrometer was operated in high-resolution mode. This setup is shown schematically in Fig. 1.

III. RESULTS

A. The distribution of cluster compositions

The use of $Co_{0.85}Mn_{0.15}$ and $Co_{0.5}Mn_{0.5}$ laser vaporization targets permitted production of Co_nMn_m cluster distributions

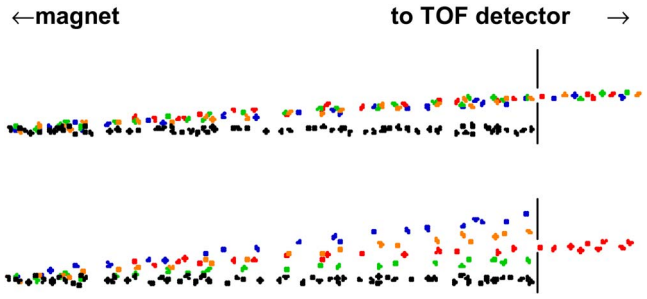

FIG. 1. (Color online) Schematic representation of beam deflection setup with a movable beamstop and slit in the beam path downbeam of the magnet. The undeflected cluster beam with the field off (shown as the horizontal beam at the bottom of each figure) strikes the beam stop. Top: With the field applied, all clusters in a given (narrow) mass range in are deflected by the same magnitude and pass through the slit to the detector. Bottom: Clusters are deflected by different magnitudes. In this case, only a subset of the clusters (e.g., those with a certain composition) are deflected through the slit.

ranging from highly cobalt rich to slightly cobalt rich (target fabrication difficulties precluded the production highly manganese-rich clusters). Magnified portions of high-mass-resolution time-of-flight spectra recorded using the $Co_{0.85}Mn_{0.15}$ and $Co_{0.5}Mn_{0.5}$ targets are shown in Fig. 2, along with a mass spectrum recorded for pure cobalt clusters. The mass spectra obtained using the Co-Mn alloy targets consist of groups of mass peaks corresponding to masses of a given $N=n+m$. The average manganese fraction $\bar{x}_{Mn}(N)$ in each group of a given N, was determined from the measured Co_nMn_m mass peak areas $I(n,m)$ corresponding to clusters possessing m manganese atoms via

$$\bar{x}_{Mn}(N) = \sum_{m=m_{min}}^{m=m_{max}} mI(n,m) \Big/ N \sum_{m=m_{min}}^{m=m_{max}} I(n,m), \qquad (1)$$

where the summation limits m_{min} and m_{max} correspond the most manganese-deficient and manganese-rich peaks measurable above the noise in the mass spectrum. The values of $\bar{x}_{Mn}(N)$ obtained using both the $Co_{0.85}Mn_{0.15}$ and $Co_{0.5}Mn_{0.5}$ targets are plotted as a function of N in Fig. 3. It can be seen that the Co_nMn_m cluster distributions are somewhat more manganese-deficient than would be expected for statistical growth (i.e., $\bar{x}_{Mn} < x_{bulk}$), particularly for smaller clusters. The propensity for the production of Co-rich Co_nMn_m clusters via co-nucleation of Co and Mn atoms has also been observed by Sone *et al.*, who used independent Co and Mn vaporization targets[30] and by Yin,[31] who used alloy target similar to those used in the present study. This phenomenon is likely the end result of differences in the nucleation rates for cobalt vs manganese atoms within the cluster source.

B. Deflection and broadening behavior

With the mass spectrometer operated in high-resolution mode, the various Co_nMn_m mass peaks are resolved even for the highest cluster group investigated ($N=29$), however, as shown in Fig. 4, operation in position-sensitive mode signifi-

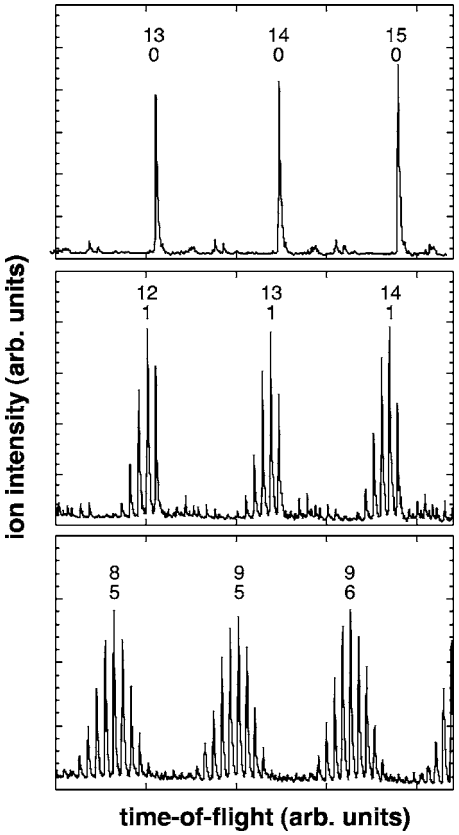

FIG. 2. Cluster time-of-flight spectra for $N=13-15$ recorded in the high-resolution (space-focusing) mode using targets of varying composition. Top: Pure cobalt; Middle: $Co_{0.85}Mn_{0.15}$; Bottom: $Co_{0.50}Mn_{0.50}$. Mass peaks are labeled according to $^{n}_{m}$.

cantly reduces the mass resolution of the instrument. This reduction in mass resolution precluded the complete separation of the individual n,m mass peaks, such that it was only possible to measure and analyze the field-induced beam deflection for a *cluster group* of given N.

Two types of beam deflection behavior were observed. At source temperatures of 90 K and above, the PSTOF mass peaks of all Co_nMn_m cluster groups produced with both the $Co_{0.85}Mn_{0.15}$ and $Co_{0.5}Mn_{0.5}$ targets shifted uniformly toward

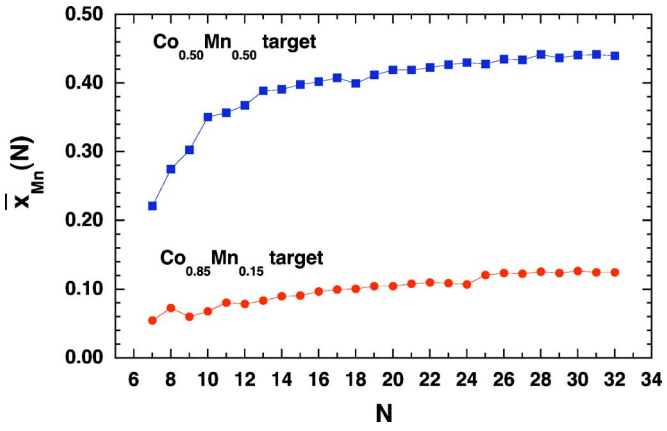

FIG. 3. (Color online) Manganese cluster fractions $\bar{x}_{Mn}(N)$ computed from mass peak intensities [see Eq. (1)].

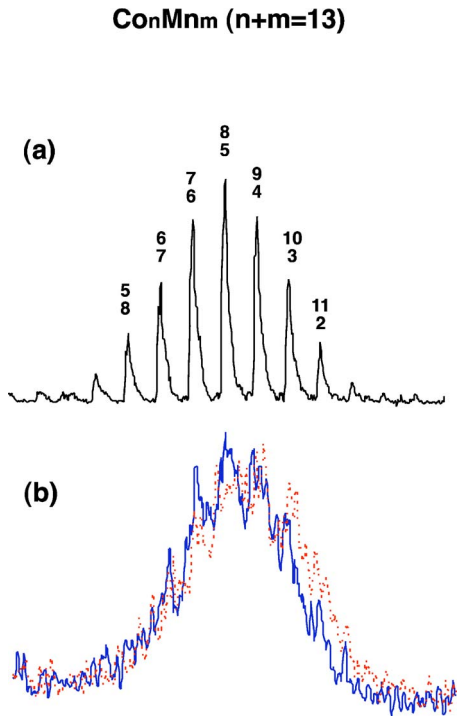

FIG. 4. (Color online) TOF profiles for Co_nMn_m $(n+m=13)$ generated with the $Co_{0.50}Mn_{0.50}$ target. Top: Space focusing mode. Mass peaks are labeled according to ^n_m. Bottom: Position sensitive mode. Solid trace, deflection field off. Dashed trace, deflection field on ($B=0.40$ T, $\partial B/\partial z=82$ T m^{-1}).

high field $(+z)$ direction, signifying superparamagnetic[32,33] (or adiabatic magnetization[34]) behavior. A qualitative change in deflection behavior was observed for at $T=55\pm5$ K for certain small, cobalt-rich cluster groups produced using the $Co_{0.85}Mn_{0.15}$ target. In particular, it was observed that the $N=9$ and 10 cluster groups produced $Co_{0.85}Mn_{0.15}$ target exhibited substantial beam broadening. This behavior indicates that some fraction of the $N=9$ and 10 clusters produced at 55 K are no longer superparamagnetic, but rather possess moments that are rigidly fixed to their molecular frameworks at they tumble through the magnet. Such behavior has been observed in small manganese clusters[5] and cobalt clusters,[35] and is analogous to the *blocked states* observed for magnetic nanoparticles at sufficiently low temperatures.[36,37]

Observation of superparamagnetic behavior allows the magnetization $\langle M_z\rangle$ of each cluster group to be determined from the magnitude of the spatial deflections, as described in detail elsewhere.[5,18] The intrinsic cluster magnetic moments μ were calculated from the measured $\langle M_z\rangle$ using the Curie Law: $\langle M_z\rangle=\mu^2B/3kT$. The justification for, and range of applicability of this thermodynamics-based analysis are discussed in detail elsewhere.[9,32,33] The mean per-atom moments $\bar{\mu}=\mu/N$ for $N=11-29$ are shown in Fig. 5 ($Co_{0.85}Mn_{0.15}$ target) and Fig. 6 ($Co_{0.50}Mn_{0.50}$ target) along with $\bar{\mu}$ values previously reported for pure Co_n clusters[35] and the predictions of the Slater-Pauling model (*vide infra*).

Because it was not possible to resolve the individual n,m mass peaks in the PSTOF spectra, the values of $\bar{\mu}$ obtained from analysis of the deflection profiles are necessarily an

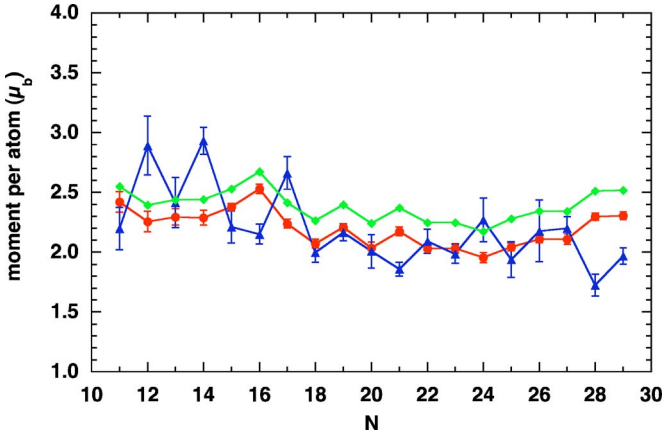

FIG. 5. (Color online) Magnetic moments per atom $\bar{\mu}$ of Co_n (●) (Ref. 35) and Co_nMn_m clusters (▲) produced with the $Co_{0.85}Mn_{0.15}$ target (this work) as a function of the total number of atoms $N=n+m$. The predictions of the Slater-Pauling model computed from the measured cluster compositions are also shown (◆). The cluster source temperatures were as follows: Pure Co_n: 150 K; Co_nMn_m 91 K.

average weighted by the $I(n,m)$ within the cluster group [see Eq. (1)]. However, qualitative information regarding the relative magnetic moments of the individual n,m species within a group N was obtained in a *differential deflection* experiment. The experiment, shown schematically in Fig. 1, was performed by positioning a beam stop containing a slit into the cluster beam between the magnet and TOF mass spectrometer, which was operated in high-resolution mode. The position of slit was adjusted slightly to the high-field $(+z)$ side of the cluster beam, such that no (or few) clusters passed to the TOF spectrometer with the deflection field off. When the deflection field was applied, a small fraction of deflected clusters in the beam passed through the slit and on to the TOF mass spectrometer where they were detected in the

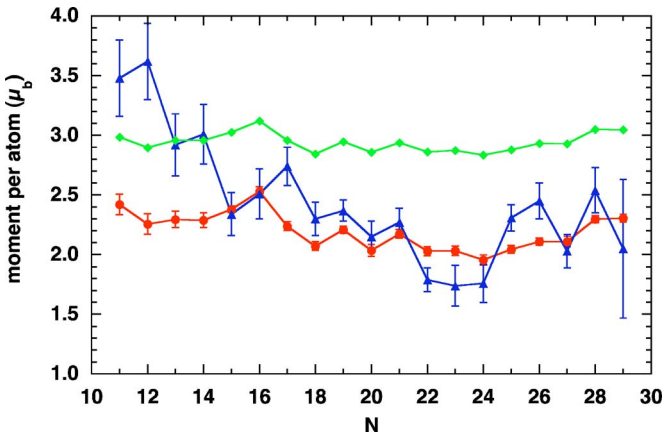

FIG. 6. (Color online) Magnetic moments per atom $\bar{\mu}$ of Co_n (●) (Ref. 35) and Co_nMn_m clusters (▲) produced with the $Co_{0.50}Mn_{0.50}$ target (this work) as a function of the total number of atoms $N=n+m$. The predictions of the Slater-Pauling model computed from the measured cluster compositions are also shown (◆). The cluster source temperatures were as follows: Pure Co_n: 150 K; Co_nMn_m 161 K.

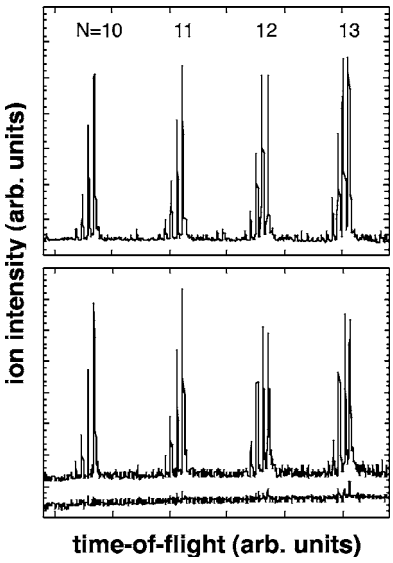

FIG. 7. High-resolution TOF spectra recorded for $N=10-13$ clusters produced using the $Co_{0.85}Mn_{0.15}$ target. Top: full-beam reference spectrum recorded with the slit and beamstop removed from the cluster beam path. Bottom: spectrum recorded using the differential deflection setup (see Fig. 1). The field-off spectrum is shown below the field-on spectrum.

usual fashion. Shown in Figs. 7 and 8 are high-resolution TOF spectra recorded for clusters produced at 90 ± 5 K using the $Co_{0.85}Mn_{0.15}$ and $Co_{0.50}Mn_{0.50}$ targets, respectively, both with no slit in the path (full beam), and with the slit positioned above the beam zero-field center line as described above. It can be seen that in both cases there are no substantial differences in the cluster intensity distributions of the full cluster beam *vs* the beams deflected through the slit. This result shows (qualitatively) that each cluster composition n,m within a group is deflected by approximately the same amount as the others regardless of manganese content, implying that moments of the various n,m species within a given group N are of the same general magnitude. Differential deflection studies of clusters produced at temperatures of 160 and 295 K produced the same qualitative result.

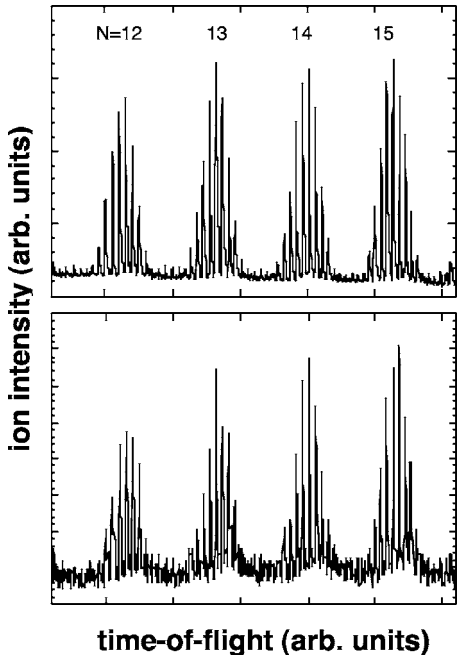

FIG. 8. High-resolution TOF spectra recorded for $N=12-15$ clusters produced using the $Co_{0.50}Mn_{05015}$ target. Top: full-beam reference spectrum recorded with the slit and beamstop removed from the cluster beam path. Bottom: spectrum recorded using the differential deflection setup (see Fig. 1).

IV. DISCUSSION

As shown in Figs. 5 and 6, the per-atom moments of the Co_nMn_m clusters are similar to or, in some cases, slightly larger than those measured[35] pure Co_n clusters. Clusters having a minority Mn content as produced with the $Co_{0.85}Mn_{0.15}$ target (see Fig. 2) have moments that are similar to those of the pure cobalt clusters having the same total number of atoms. Likewise, clusters produced with the $Co_{0.50}Mn_{0.50}$ target are of similar magnitude as the corresponding pure Co_n clusters, except for $N=11-14$ clusters, which possess moments that are somewhat larger. These results show that Mn-for-Co substitution does not lead to a substantial change in cluster moments. This conclusion is supported by the differential deflection experiments (Figs. 7 and 8), in which it is seen that the n,m distributions of the deflected clusters are similar to the full-beam distributions recorded with the deflection field off.

That Mn-for-Co substitution does not lead to a substantial net change in cluster magnetic moments is a result that would not be anticipated based on the magnetic properties of the bulk alloys.[38–48] At $T=150$ K, bulk $Co_{1-x}Mn_x$ alloys display susceptibilities[44,48–50] in the range $1-3\times10^{-3}$, reflecting a variety of nonferromagnetic phases including ferromagnetic short-range order ($x=0.25-0.30$), paramagnetism ($x=0.30-0.35$), antiferromagnetic short-range order ($x=0.35-0.43$) and antiferromagnetism ($x>0.43$).[47,51] Although the boundaries between these various magnetic phases vary somewhat with temperature, susceptibilities of similar magnitude are observed within this range of compositions from $T=0$ K to 400 K.[44,48,49]

Both cobalt and manganese are magnetically ordered as solids: Cobalt is ferromagnetic up to 1388 K, whereas manganese is antiferromagnetically ordered up to 95 K.[20,52] Neutron scattering studies of $Co_{1-x}Mn_x$ alloys have been used to determine the variation individual atomics moments μ_{Co} and μ_{Mn} with increasing Mn:Co ratio. The results are summarized in Fig. 9. On the cobalt-rich side of the phase diagram the atomic moments of Co and Mn are aligned antiferromagnetically, with the magnitude of both μ_{Co} and μ_{Mn} decreasing montonically with increasing Mn content such that the mean per-atom moment of the alloy $\bar{\mu}=x\mu_{Co}+(1-x)\mu_{Mn}$ also decreases strongly with Mn content,[44,47,51] from $\bar{\mu}=1.72\mu_b$ at $x=0$ to $\bar{\mu}=0\mu_b$ at $x=0.32$.[44] Accompanying the decrease in $\bar{\mu}$ with increasing Mn content is a monontonic decrease in the ordering temperature, from 1388 K for $x=0$ to ~0 K for $x=0.25$.[44,51] $Co_{1-x}Mn_x$ alloys deviate strongly from the Slater-Pauling (S-P) model[53] of $3d$ alloy itinerant ferromag-

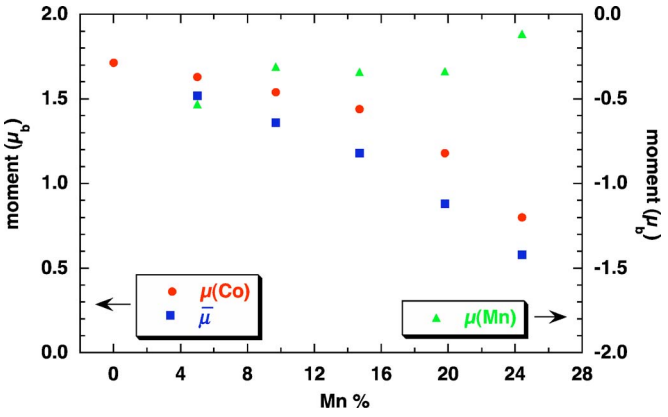

FIG. 9. (Color online) Magnetic moments μ_{Co}, μ_{Mn}, and $\bar{\mu}=(1-x)\mu_{Co}+x\mu_{Mn}$ for bulk $Co_{1-x}Mn_x$ alloys as determined from neutron scattering. The negative sign for μ_{Mn} signifies its antiferromagnetic alignment with respect to μ_{Co}.

netism, in which simple valence electron counting rules in conjunction with the rigid-band assumption is used to predict the average magnetic moment $\bar{\mu}$ as a function of composition. When applied to the $Co_{1-x}Mn_x$ system, the S-P model predicts an incremental increase in the average moment $\bar{\mu}$ upon Mn-for-Co substitution: $(\partial\bar{\mu}/\partial x)_{x\to 0}=+2\mu_b$. This prediction is clearly at odds with what has been determined experimentally for $Co_{1-x}Mn_x$ alloys.

Co_nMn_m clusters possessing susceptibilities of the same magnitude as those of the non-ferromagnetic $Co_{1-x}Mn_x$ bulk phases would display unmeasurably small spatial deflections and thus yield near-zero moments in the present experiment. The magnitude of the measured Co_nMn_m moments indicate that they are ferromagnetically (or ferrimagnetically) ordered at temperatures and compositions at which the corresponding bulk alloys are not. Unlike bulk $Co_{1-x}Mn_x$ alloys in which the presence of Mn decreases the mean per-atom moments, the presence of a significant fraction of manganese in small Co_nMn_m clusters results in overall moments that are comparable those of the corresponding pure Co_n clusters, and in some cases (e.g., $N=11-14$) larger. This suggests that, unlike the bulk alloys of similar composition, both Co and Mn constituents within the clusters retain substantial moments even at high Mn fractions. The predictions of the S-P model as applied to Co_nMn_m clusters are shown in Figs. 5 and 6 together with the experimentally determined average moments $\bar{\mu}$. The S-P model was applied using the experimentally determined moments[35] of the pure cobalt cluster "hosts" and the experimentally determined compositions. As shown in Fig. 5, the moments predicted by the S-P model for cobalt-rich clusters are only slightly larger than those of both the pure Co_n clusters and Co_nMn_m clusters generated using the $Co_{0.85}Mn_{0.15}$ target. However, as shown in Fig. 6, the S-P model significantly overestimates the moments of the Co_nMn_m clusters containing a substantial fraction of manganese, as generated using the $Co_{0.50}Mn_{0.50}$ target. The assumptions inherent in the S-P model (rigid host d-band, composition-independent moments, strictly ferromagnetic coupling) limit its value in the present case to (at best) qualitative predictions. In the absence of detailed electronic structure calculations of Co_nMn_m clusters, the magnitude of the Co and Mn moments and nature of the coupling between them remains unclear.

Insight into the electronic structures of Co_nMn_m clusters can be gleaned from the corresponding diatomic molecule, CoMn, which is well characterized. Formation of the cobalt dimer, Co_2, from the ground state ($3d^74s^2$, $^4F_{9/2}$) atoms leads to an effective $4s^{1.0}3d^{8.0}$ electronic configuration as a result of $4s\to 3d$ promotion.[54] The resulting $^5\Delta_g$ ground state of Co_2 ground state possesses a net spin $S=2$. By contrast the $^7\Delta$ ground state of CoMn possesses a net spin $S=3$, with effective atomic configurations $4s^{1.02}3d^{8.12}$ (Co) and $4s^{1.03}3d^{5.77}$ (Mn).[55] In simple terms, substitution of Mn-for-Co leads to a net reduction of approximately two d electrons in the diatomic molecule. Density functional calculations show that these two electrons occupied minority (β) spin-orbitals centered on the atoms.[55] Their "removal" upon Mn-for-Co substitution thus leads to a net increase in spin from 2 to 3, and thus an increase in spin moment from $4\mu_b$ to $6\mu_b$. This $2\mu_b$ increase in spin moment is in qualitative accord with the present results and in reasonable quantitative agreement the $+1.7\mu_b$ change measured for Mn-for-Co substitution Co_nMn_m clusters by Yin.[31] The angular momentum coupling situation in polyatomic Co_nMn_m clusters is obviously more complex than this simple diatomic model would suggest, however (orbital moments will likely be fully or partially quenched, for example). Electronic structure and thus magnetism will likely be critically dependent on cluster geometries and spatial arrangements of Co vs Mn atoms. For example, clusters in which Mn and Co constituents are segregated can be expected to have significantly different magnetic properties than those in which they are mixed. Calculations of equilibrium structures (including isomers) and their corresponding properties will be required for a complete understanding of the Co_nMn_m system.

ACKNOWLEDGMENTS

This work is supported by the U.S. Department of Energy, Office of Basic Energy Sciences, Division of Chemical Sciences, under Contract No. DE-AC02-06CH11357 and by the CREST (Core Research for Evolutional Science and Technology) program of the Japan Science and Technology Agency (JST). Illuminating discussions with Walt de Heer and Shuangye Yin are gratefully acknowledged.

[1] A. J. Cox, J. G. Louderback, and L. A. Bloomfield, Phys. Rev. Lett. **71**, 923 (1993).
[2] A. J. Cox, J. G. Louderback, S. E. Apsel, and L. A. Bloomfield, Phys. Rev. B **49**, 12295 (1994).
[3] L. A. Bloomfield, J. Deng, H. Zhang, and J. W. Emmert, in *Proceedings of the International Symposium on Cluster and Nanostructure Interfaces*, edited by P. Jena, S. N. Khanna, and B. K. Rao (World Publishers, Singapore, 2000), p. 131.
[4] M. B. Knickelbein, Phys. Rev. Lett. **86**, 5255 (2001).
[5] M. B. Knickelbein, Phys. Rev. B **70**, 014424 (2004).
[6] M. B. Knickelbein, Phys. Rev. B **71**, 184442 (2005).
[7] Y. Qiang, R. F. Sabiryanov, S. S. Jaswal, Y. Liu, H. Haberland, and D. J. Sellmyer, Phys. Rev. B **66**, 064404 (2002).
[8] C. Binns, M. J. Maher, Q. A. Pankhurst, D. Kechrakos, and K. N. Trohidou, Phys. Rev. B **66**, 184413 (2002).
[9] J. P. Bucher and L. A. Bloomfield, Int. J. Mod. Phys. B **7**, 1079 (1993).
[10] J. P. Bucher, D. C. Douglass, and L. A. Bloomfield, Phys. Rev. Lett. **66**, 3052 (1991).
[11] I. M. L. Billas, A. Châtelain, and W. A. de Heer, Science **265**, 1682 (1994).
[12] I. M. L. Billas, A. Châtelain, and W. A. de Heer, J. Magn. Magn. Mater. **168**, 64 (1997).
[13] A. Châtelain, Philos. Mag. B **79**, 1367 (1999).
[14] D. Gerion, A. Hirt, and A. Châtelain, Phys. Rev. Lett. **83**, 532 (1999).
[15] D. Gerion, A. Hirt, I. M. L. Billas, A. Châtelain, and W. A. de Heer, Phys. Rev. B **62**, 7491 (2000).
[16] S. Pokrant and J. A. Becker, J. Magn. Magn. Mater. **226–230**, 1921 (2001).
[17] T. Hihara, S. Pokrant, and J. A. Becker, Chin. Phys. Lasers **294**, 357 (1998).
[18] M. B. Knickelbein, J. Chem. Phys. **116**, 9703 (2002).
[19] J. Bansmann, S. H. Baker, C. Binns, J. A. Blackman, J.-P. Bucher, J. Dorantes-Dávila, V. Dupuis, L. Favre, D. Kechrakos, A. Kleibert, K. H. Meiwes-Broer, G. M. Pastor, A. Perez, O. Toulemonde, K. N. Trohidou, J. Tuaillon, and Y. Xie, Surf. Sci. Rep. **56**, 189 (2005).
[20] K. Adachi, D. Bonnenberg, J. J. M. Franse, R. Gersdorf, K. A. Hempel, K. Kanematsu, S. Misawa, M. Shiga, M. B. Stearns, and H. P. J. Wijn, in *Landolt-Börnstein*, edited by H. P. J. Wijn (Springer-Verlag, Berlin, 1986), Vol. 19.
[21] S. Yin, X. Xu, R. Moro, and W. A. de Heer, Phys. Rev. B **72**, 174410 (2005).
[22] G. M. Koretsky, K. P. Kerns, G. C. Nieman, M. B. Knickelbein, and S. J. Riley, J. Phys. Chem. A **103**, 1997 (1999).
[23] M. B. Knickelbein, S. Yang, and S. J. Riley, J. Chem. Phys. **93**, 94 (1990).
[24] B. A. Collings, A. Amrein, D. M. Rayner, and P. A. Hackett, J. Chem. Phys. **99**, 4174 (1993).
[25] D. McColm, Rev. Sci. Instrum. **37**, 1115 (1966).
[26] M. B. Knickelbein and S. Yang, J. Chem. Phys. **93**, 5760 (1990).
[27] S. Yang and M. B. Knickelbein, J. Chem. Phys. **93**, 1533 (1990).
[28] J. L. Persson, Ph.D. thesis, University of California, Los Angeles, 1991.
[29] W. A. de Heer and P. Milani, Rev. Sci. Instrum. **62**, 670 (1991).
[30] Y. Sone, K. Hoshino, T. Naganuma, A. Nakajima, and K. Kaya, J. Phys. Chem. **95**, 6830 (1991).
[31] S. Yin, Ph.D. thesis, Georgia Insitute of Technology, 2006.
[32] S. N. Khanna and S. Linderoth, Phys. Rev. Lett. **67**, 742 (1991).
[33] M. B. Knickelbein, J. Chem. Phys. **121**, 5281 (2004).
[34] X. Xu, S. Yin, R. Moro, and W. A. de Heer, Phys. Rev. Lett. **95**, 237209 (2005).
[35] M. B. Knickelbein, J. Chem. Phys. **125**, 044308 (2006).
[36] S. A. Majetich, J. H. Scott, E. M. Kirkpatrick, K. Chowdary, K. Gallagher, and M. E. McHenry, Nanostruct. Mater. **9**, 291 (1997).
[37] Clusters whose moments are fixed to their molecular framework as they tumble through the magnet are sometimes characterized as having "locked moments."
[38] J. Crangle, Philos. Mag. **2**, 659 (1957).
[39] R. Hahn and E. Kneller, Z. Metallkd. **49**, 426 (1958).
[40] K. Adachi, K. Sato, M. Matsui, and S. Mitani, J. Phys. Soc. Jpn. **25**, 426 (1973).
[41] J. W. Cable and T. J. Hicks, Phys. Rev. B **2**, 176 (1970).
[42] Y. Koi, A. Tsujimura, T. Hihara, and T. Kushida, J. Phys. Soc. Jpn. **16**, 574 (1961).
[43] J. S. Kouvel, J. Phys. Chem. Solids **16**, 107 (1960).
[44] M. Matsui, T. Ido, K. Sato, and K. Adachi, J. Phys. Soc. Jpn. **28**, 791 (1970).
[45] M. Matsui, K. Sato, and K. Adachi, J. Phys. Soc. Jpn. **35**, 419 (1973).
[46] M. Mekata, Y. Nakahashi, and T. Yamaoka, J. Phys. Soc. Jpn. **37**, 1509 (1974).
[47] J. W. Cable, Phys. Rev. B **25**, 4670 (1982).
[48] D. R. Rhiger, D. Müller, and P. A. Beck, J. Magn. Magn. Mater. **15-18**, 165 (1980).
[49] T. Hori, J. Phys. Soc. Jpn. **38**, 1780 (1975).
[50] Here we have converted published mass susceptibilities to dimensionless susceptibilities, expressed in the SI convention.
[51] A. Z. Men'shikov, G. A. Takzeï, Y. A. Dorofeev, V. A. Kazantsev, A. K. Kostyshin, and I. I. Sych, Sov. Phys. JETP **62**, 734 (1985).
[52] E. P. Wohlfarth, in *Ferromagnetic Materials*, edited by E. P. Wohlfarth (North-Holland, Amsterdam, 1980), Vol. 1, p. 1.
[53] D. Jiles, *Magnetism and Magnetic Materials* (Chapman and Hall, London, 1998).
[54] G. L. Gutsev and C. W. Bauschlicher, Jr., J. Phys. Chem. A **107**, 4755 (2003).
[55] G. L. Gutsev, M. D. Mochena, P. Jena, C. W. Bauschlicher, Jr., and H. Partridge III, J. Chem. Phys. **121**, 6785 (2004).